Neuroscience 252 (2013) 443–459

LOCALIZATION OF α7 NICOTINIC ACETYLCHOLINE RECEPTOR IMMUNOREACTIVITY ON GABAERGIC INTERNEURONS IN LAYERS I–III OF THE RAT RETROSPLENIAL GRANULAR CORTEX

K. MURAKAMI,* Y. ISHIKAWA AND F. SATO

Department of Anatomy, Toho University School Medicine, Omori-nishi 5-21-16, Ota-ku, Tokyo 143-8540, Japan

Abstract—The rat retrosplenial granular cortex (RSG) receives cholinergic input from the medial septum–diagonal band (MS–DB) of the cholinergic basal forebrain (CBF), with projections terminating in layers I–III of RSG. The modulatory effects of acetylcholine (ACh) on cortical GABAergic interneurons in these layers are mediated by α7 nicotinic acetylcholine receptors (α7nAChRs). α7nAChRs are most abundant in the cerebral cortex and are largely localized to GABAergic interneurons. However, the CBF projection to the RSG has not been studied in detail, and the cellular or subcellular distribution of α7nAChRs in the rat RSG remains unclear. The main objective of this study was to test that α7nAChRs reside on GABAergic interneurons in CBF terminal fields of the rat RSG. First, we set out to define the characteristics of CBF projections from the MS–DB to layers of the RSG using anterograde neural tracing and immunohistochemical labeling with cholinergic markers. These results revealed that the pattern of axon terminal labeling in layer Ia, as well as layer II/III of the RSG is remarkably similar to the pattern of cholinergic axons in the RSG. Next, we investigated the relationship between α7nAChRs, labeled using either α-bungarotoxin or α7nAChR antibody, and the local neurochemical environment by labeling surrounding cells with antibodies against glutamic acid decarboxylase (GAD), parvalbumin (PV) and reelin (a marker of the ionotropic serotonin receptor-expressing GABAergic interneurons). α7nAChRs were found to be localized on both somatodendritic and neuronal elements within subpopulations of GABAergic PV-, reelin-stained and non PV-stained neurons in layers I–III of the RSG. Finally, electron microscopy revealed that α7nAChRs are GAD- and PV-positive cytoplasmic and neuronal elements. These results strongly suggest that ACh released from CBF afferents is transmitted via α7nAChR to GAD-, PV-, and reelin-positive GABAergic interneurons in layers I–III of the RSG.

Key words: retrosplenial granular cortex, α7nAChR, GABAergic interneuron, parvalbumin, cholinergic basal forebrain.

INTRODUCTION

The retrosplenial granular cortex (RSG) is a portion of the retrosplenial cortex (RSC) defined by its cellular architecture. The RSC, which has been separated into granular (areas 29a–c) and agranular (area 30) areas in the rat, occupies the caudal half of the cingulate cortex (Vogt and Peters, 1981; Vogt and Miller, 1983). The rat RSG is distinguished from the retrosplenial agranular area by its distinctly organized granular layer (Vogt et al., 2004). Although the RSG consists of three areas (29a–c), in the present study, we have limited our investigation to area 29c, because this area projects heavily to, and receives afferent inputs from the hippocampal formation, and the anteroventral and anterodorsal thalamic nuclei, which are brain areas involved in emotion and episodic memory (Aggleton and Brown, 1999; Maddock, 1999; Aggleton and Pearce, 2001; Aggleton, 2010).

It is now evident that the RSG plays an important role in a range of cognitive functions, including spatial learning, memory and navigation in rodents (Cooper and Mizumori, 1999, 2001; Cooper et al., 2001; Harker and Whishaw, 2002; Vann and Aggleton, 2002; Vann et al., 2003, 2009; van Groen et al., 2004; Garden et al., 2009). These diverse functions are thought to be mediated by thalamic (Robertson and Kaitz, 1981; Sripanidkulchai and Wyss, 1986; van Groen and Wyss, 1990, 1992; Vogt et al., 1992; Shibata et al., 2004), basal forebrain (Price and Stern, 1983; Finch et al., 1984; Mufson and Pandya, 1984; Saper, 1984; Gaykema et al., 1990; White and Tan, 1991; Tengelsen et al., 1992; Gonzalo-Ruiz and Morte, 2000; Murakami et al., 2000; Robertson et al., 2009), hippocampal CA1 (Wyss and Van Groen, 1992; Cenquizca and Swanson, 2007; Jinno et al., 2007; Miyashita and Rockland, 2007), and subiculum projections to the RSG (Sorensen, 1980; Vogt and Miller, 1983). In particular, studies of

*Corresponding author. Tel: +81-3-3762-4151x2313; fax: +81-3-5493-5411.
E-mail address: kunim@med.toho-u.ac.jp (K. Murakami).

Abbreviations: α7nAChRs, α7 nicotinic acetylcholine receptors; αBTX, α-bungarotoxin; Aβ, β-amyloid; ACh, acetylcholine; AD, Alzheimer's disease; BSA, 1% bovine serum albumin; CBF, cholinergic basal forebrain; ChAT, choline acetyltransferase; CHT, high affinity choline transporter; DAB, 0.22% 3,3-diaminobenzidine; FS, fast-spiking; GAD, glutamic acid decarboxylase; GAD, anti-GAD65 and 67; GAD-ip, GAD-ir identified by DAB reaction product; HDBm, medial part of the horizontal limb of the diagonal band of Broca; 5HT3a, ionotropic serotonin receptor; MS–DB, medial septum–diagonal band; NGS, 5% normal goat serum; p75, p75 neurotrophin receptor; PB, 0.1 M sodium phosphate buffer (pH 7.4); PBS, PB saline; PFA, paraformaldehyde; PHA-L, *Phaseolus vulgaris* leucoagglutinin; PV, parvalbumin; PV-ip, PV-ir identified by DAB reaction product; RSC, retrosplenial cortex; RSG, retrosplenial granular cortex; TBS, 0.05 M Tris–HCl-buffered saline; Tg-Alz mice, transgenic AD mice; vAChT, vesicular acetylcholine transporter.

0306-4522/13 $36.00
http://dx.doi.org/10.1016/j.neuroscience.2013.08.024

retrograde neural tracing combined with immunohistochemistry have revealed that the rat RSG receives cholinergic input from the medial septum–diagonal band complex (MS–DB) of the cholinergic basal forebrain (CBF) (Rye et al., 1984; Senut et al., 1989; Tengelsen et al., 1992; Gonzalo-Ruiz and Morte, 2000). In addition, studies using anterograde neuronal tracing have shown that projections from the MS–DB terminate in layer III of the RSG (Saper, 1984; Gaykema et al., 1990; Murakami et al., 2000; Robertson et al., 2009).

Recent studies have reported that the RSC, as well as the hippocampal–parahippocampal regions show progressive atrophy in Alzheimer's disease (AD; Villain et al., 2008; Pengas et al., 2010). Furthermore, there is evidence of functional abnormalities in amyloid precursor protein-derived peptide accumulation and of c-Fos hyperactivity during the early stages of AD in transgenic mice (Tg-Alz mice; Irizarry et al., 1997; McGowan et al., 1999; Takeuchi et al., 2000; Poirier et al., 2011). Additionally, β-amyloid (Aβ) deposits occur in layer III of the RSG of triple Tg-Alz mice (Robertson et al., 2009). Aβ is thought to be a causal factor in AD and binds with high affinity to the α7 nicotinic acetylcholine receptor (α7nAChR: Wang et al., 2000a,b).

α7nAChRs are most abundant in the hippocampus and neocortex and are strongly expressed in GABAergic interneurons (Alkondon et al., 1997; Frazier et al., 1998a,b; McQuiston and Madison, 1999; Ji and Dani, 2000); the receptor complex is highly permeable to calcium (Dajas-Bailador and Wonnacott, 2004). α7nAChRs are also abundantly expressed in basal forebrain cholinergic neurons projecting to the hippocampus and cortex, correlating well with brain areas that develop neuritic plaques in AD. Additionally, recent studies have demonstrated evoked synaptic currents in hippocampal interneurons, which are mediated by post- and extrasynaptic α7nAChRs (Alkondon et al., 1998, 1999; Frazier et al., 1998a,b), suggesting that both pre- and postsynaptic α7nAChRs play a significant role in the cholinergic modulation of neurotransmission.

However, in contrast to brain regions such as the hippocampus, the RSG is poorly understood, and it is uncertain whether RSG interneurons receiving cholinergic inputs express nicotinic receptors. In the rat RSG, GABAergic parvalbumin (PV)-labeled neural elements are primarily evident in the outer molecular layer and layers II–III and form columnar arrangements bridging these layers (Ichinohe and Rockland, 2002; Ichinohe, 2012). Because these interneurons project to pyramidal neurons as well as other interneurons, activation of the cholinergic system is likely to produce a complex modulation of local inhibitory activity (Kawaguchi, 1997; Porter et al., 1999; Buhler and Dunwiddie, 2001). However, the cellular and subcellular distribution of α7nAChRs in the rat RSG remains unclear, although many modulatory effects of cortical GABAergic interneurons are mediated by α7nAChRs. In CBF terminal fields of the rat RSG, the distribution of CBF terminals remains unclear.

The present study was performed in order to define the characteristics of projections from the MS–DB complex to layers of the RSG using anterograde neural tracing with *Phaseolus vulgaris* leucoagglutinin (PHA-L), and the immunohistochemical detection of several cholinergic markers; namely, choline acetyltransferase (ChAT), the vesicular acetylcholine transporter (vAChT), the high affinity choline transporter (CHT), and p75 neurotrophin receptor (p75). In order to elucidate the relationship between α7nAChR (labeled with the specific antagonist α-bungarotoxin (αBTX) or the α7nAChR antibody) and the local neurochemical environment of receptor binding sites in layers I–III of the RSG, we applied multiple labeling strategies with antibodies against glutamic acid decarboxylase (GAD), PV and reelin, which was recently reported as a marker of the ionotropic serotonin receptor (5HT3a)-expressing GABAergic interneurons (Miyoshi et al., 2010). Finally, to determine the location of the α7nAChR within GABAergic neural elements of the RSG, we used electron microscopy to examine the immunolabeling of α7nAChR, and GAD or PV, in single sections through the RSG.

Here, we report the localization of α7nAChRs in layers I–III of the rat RSG, and the relationship between acetylcholine (ACh) released from the CBF and GABAergic interneurons in layers I–III of the rat RSG. Our findings provide evidence that ACh carries a diffuse signal in the superficial layers of the RSG and is likely to modulate inhibitory neurotransmission among interneurons.

EXPERIMENTAL PROCEDURES

Animals

All procedures were performed in accordance with the guidelines for animal welfare established by the animal welfare committees of Toho University, which include all adequate measures to minimize pain or discomfort. A total of 10 male Wistar rats weighing 290–310 g were used in the present study.

Anterograde tracing experiments and preparation for PHA-L labeling

Three rats were anesthetized with intraperitoneal injections of xylazine (10 mg/kg body weight) and ketamine (50 mg/kg body weight) in preparation for surgery. Unilateral iontophoretic injections of 2.5% PHA-L in 0.1 M sodium phosphate buffer (pH 7.4: PB) were administered to the medial part of the horizontal limb of the diagonal band of Broca (HDBm) and the anterior division of the substantia innominata (Fig. 1A). Coordinates were taken from a bregma according to the Paxinos and Watson stereotaxic atlas (1998). PHA-L solution was back-filled into a glass micropipette with a 20-μm internal diameter. Iontophoretic injections into the HDBm were performed using an intermittent current of 5–7 μA, with 7-s on/off cycle for 20 min. After a survival time of 7 days, the rats were deeply anesthetized with Nembutal (80 mg/kg body weight, i.p.), and perfused

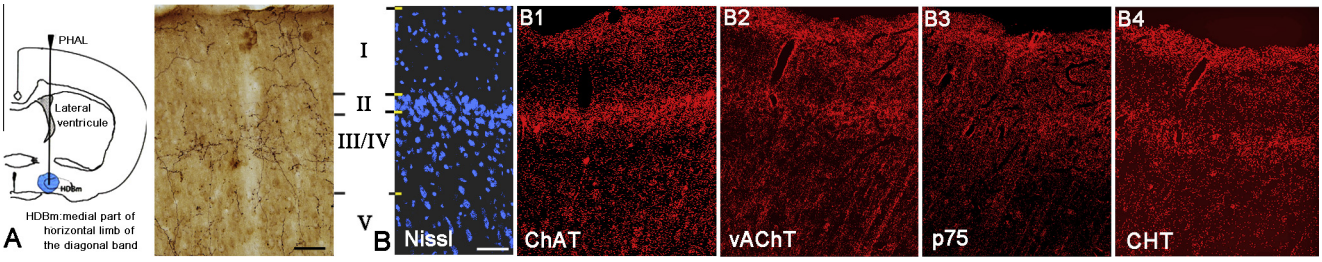

Fig. 1. (A) Photomicrograph showing basalocortical PHA-L-labeled fibers in the retrosplenial granular cortex (RSG) following a series of injections of PHA-L into the medial part of the horizontal limb of the diagonal ban (HDBm). PHA-L labeled fibers are concentrated in layers I and III of the retrosplenial cortex. (B) Immunostaining for several cholinergic antibodies (B1: ChAT, B2: vACh, B3: p75, B4: CHT) in the RSG. Cholinergic fibers expressing the various specific antibodies are numerous in layers Ia and II–III of the RSG. Nissl staining: blue. Scale bar = 50 μm.

through the aorta with heparinized saline (100 units/ml) followed by 400–600 ml of a mixture containing 4% paraformaldehyde (PFA) in PB. The brain was dissected, and sections were cut in the coronal plane through the RSG at 50-μm thickness on a microslicer (Dosaka EM Co., Kyoto, Japan).

The steps for PHA-L labeling were carried out in 0.1 M PB saline solution containing 0.3% Triton-X (PBS-X). Following a freeze–thaw procedure using liquid nitrogen to enhance the penetration of antibodies, sections were pretreated for 1 h in a blocking solution (BS) containing 5% normal goat serum (NGS: Chemicon, Temecula, CA, USA) and 1% bovine serum albumin (BSA: Sigma–Aldrich Co. St. Louis, MO, USA) in PBS. Sections were then incubated with the primary antibody solution containing rabbit anti-PHA-L antibody (1:1000; Vector Laboratories, Burlingame, CA, USA) in BS at 4 °C for 48 h. A second incubation was performed for 1 h at room temperature (RT) with biotinylated goat anti-rabbit IgG (1:100; Vector Lab.) in BS. Sections were then transferred for 1 h into an ABC reagent (1:100; Vectastain *Elite* Kit; Vector Lab.). Following three successive rinses in PBS and in 0.05 M Tris–HCl-buffered saline (TBS) at pH 7.6, sections were exposed to a solution of 0.22% 3,3-diaminobenzidine (DAB), 0.003% H2O2 in 0.05 M TB at pH 7.6. Stained sections were then mounted onto gelatin-coated slides, dehydrated, and coverslipped with Permount (Fisher Scientific, Fair Lawn, NJ, USA).

Preparation for immunofluorescence and electron microscopy

Seven male Wistar rats (B.W. 290–310 g) were deeply anesthetized by an intraperitoneal injection of pentobarbital (10 mg/kg) and perfused transcardially with a solution of 4% PFA in PB for light microscopy, or 3.75% acrolein and 2% PFA for electron microscopy. Brains were then removed from the skull and cut into several blocks. The blocks were postfixed with 2% PFA for 2–3 h at 4 °C and rinsed with PB. For immunofluorescence, blocks were equilibrated in a 25% sucrose solution, and 35-μm-thick sections were cut using a freezing microtome. Sections were washed thrice for 10 min each in PB, and then incubated in PB containing 1% sodium borohydride for 10 min in order to reduce residual aldehyde groups. Specimens were then stored at −20 °C in antifreeze solution (0.01 M NaH_2PO_4, 0.03 M Na_2HPO_4, 30% ethylene glycol, and 30% glycerol) until use.

Immunofluorescence staining for cholinergic markers

Sections were incubated for 1 h in BS (containing 0.1% Triton X-100 and 1% BSA, and either 5% NGS or 5% normal donkey serum [Chemicon] in PBS), at RT, and then incubated for 48–72 h at 4 °C in the primary antibody solution containing the cholinergic markers for either mouse anti-ChAT (1:500; Chemicon), goat anti-vAChT (1:1000; Promega, Madison, WI, USA), rabbit anti-CHT (1:500; Chemicon), or rabbit anti-p75 (1:1000; Promega), diluted in BS. After rinsing, the sections were placed in BS containing a fluorophore-conjugated secondary antibody; either Cy3-goat anti-mouse (1:100; Zymed, South San Francisco, CA, USA), Cy3-donkey anti-goat (1:100; Jackson ImmunoResearch, West Grove, PA, USA), or Cy3-donkey anti-rabbit (1:100; Chemicon) for 2 h at RT. Following further rinsing, all sections were mounted onto gelatin-coated slides, dried, and coverslipped in DAPI-fluoromount-G (SouthernBiotech, Birmingham, AL, USA).

Double immunolabeling for GABAergic markers and α7nAChR

The specificity of the mouse anti-α7nAChR antibody has been previously demonstrated by several in mouse, rat, and macaque brain extracts (Dominguez Del Toro et al., 1994; Centeno et al., 2006; Arnaiz-Cot et al., 2008; Duffy et al., 2009).

For immunolabeling, free-floating sections were pre-incubated in BS (containing 5% NGS, 2% BSA, and 0.05% Triton X-100 in PBS) at RT for 3 h in order to reduce background signal. Sections were then incubated in BS containing a monoclonal anti-α7nAChR antibody, Mab 306 (1:1000; Sigma), and either a polyclonal rabbit anti-GAD65 and 67 (1:500; Chemicon) or a polyclonal rabbit anti-PV (1:500; ImmunoStar, Hudson, WI, USA) at 4 °C for 5 days on a rotary shaker. After washing in PBS, sections were incubated for 48 h at 4 °C in BS containing the fluorophore-conjugated secondary antibodies Cy3-goat anti-mouse (1:250; Zymed) and Cy2-goat anti-rabbit (1:250; Jackson).

Labeling for GABAergic markers and αBTX

Immunolabeling with antisera against α7-nAChR was confirmed by histochemical staining with the α7nAChR-specific antagonist α-bungarotoxin. Tissue sections were washed in PBS at pH 7.4 (3 × 10 min), and non-specific binding sites were blocked by incubation in BS (containing 5% 5% normal donkey serum (NDS), 2% BSA, and 0.05% Triton X-100 in PBS) for 2 h. Sections were rinsed in PBS and then incubated in 10 nM Alexa488-conjugated αBTX (1:500; Molecular Probes, Eugene, OR, USA) at 4 °C for 5 days.

To visualize the association between αBTX binding sites and GABAergic interneurons in the RSG, three primary antibodies were added to the BS. These were directed against GABAergic cortical interneurons and neuropiles (rabbit anti-GAD, anti-PV and mouse anti-reelin (1:500; Calbiochem, Merck KGaA, Darmstadt, Germany), respectively). After washing in PBS (5 × 10 min), preparations were incubated overnight at 4 °C in BS containing Cy3 donkey anti-rabbit (1:100; Chemicon) or Cy3 donkey anti-mouse (1:100; Jackson), and Alexa488-conjugated αBTX (1:500, see above). After washing in PBS, sections were mounted in DAPI-fluoromount-G on glass slides and examined using either a Zeiss microscope equipped with epi-fluorescence illumination or a Zeiss LSM510 Meta confocal microscope. Images were digitally captured, pseudocolored, and merged using either Adobe Photoshop software or the Zeiss confocal software. Light microscopy figures were assembled using Adobe Photoshop.

Immunocytochemical and specific αBTX labeling controls

The specificity of the secondary antibodies used was evaluated by the omission of the primary antibodies from each immunoreaction. These sections produced labeling which was consistent with each label individually. In addition, in some cases the sequence of labeling or the method of detection was varied to ensure that results remained consistent. The αBTX conjugates used in this study have been previously shown to be specific for α7nAChRs in comparable labeling studies, by competition with α7nAChR-specific antagonists such as unconjugated αBTX (Kawai et al., 2002; Jones and Wonnacott, 2004). Pre-incubation of sections with an excess of unconjugated αBTX (data not shown) eliminated fluorescent αBTX labeling, demonstrating that the fluorescent αBTX conjugate binds specifically to α7nAChRs.

Processing for pre-embedding immunoelectron microscopy

For electron microscopy, after post-fixation, 40- to 50-μm-thick coronal sections through the RSG were cut using a vibratome. Sections were placed in 1% sodium borohydride in 0.1 M PB for 30 min in order to remove reactive aldehydes. Sections were then stored at −70 °C in storage solution until use, and were freeze–thawed thrice using liquid nitrogen to enhance the penetration of antibodies. The sections were then washed in 0.1 M PB, and incubated in a BS containing 0.2% BSA, and 3% NGS in 0.02 M PBS for 30 min, as previously described (Sesack et al., 1998). Sections were incubated first in α7nAChR antibody (1:500) for 48 h at 4 °C. Following this, GAD (1:5000) or PV antibody (1:8000) was added to the solution, and the incubation continued for an additional 72 h. After incubation with the primary antisera, tissue sections were rinsed in PBS and processed for immunogold labeling of α7nAChR and immunoperoxidase labeling of GAD or PV.

To visualize α7nAChR, sections were processed using the silver-enhanced immunogold technique (Chan et al., 1990). For this, sections were rinsed four times for 10 min in PBS and incubated in a 1:50 dilution of goat anti-rabbit IgG conjugated to 0.8 nm gold particles (Aurion, Wageningen, Netherlands) in 0.1% cold fish gelatin (Sigma), 0.5% NGS, and 0.08% BSA in PBS overnight at 4 °C. Sections were then rinsed in PBS, post-fixed in 1.25% glutaraldehyde in PBS for 10 min, and rinsed again with PBS, followed by 0.2 M sodium citrate buffer at pH 7.4.

Throughout all incubations and washes, sections were continuously agitated on a rotary shaker. Nanogold particles were subsequently enhanced using a Goldenhance kit (Aurion) for 7 min. Sections were then washed four times for 10 min in Ultra-DW, and twice for 10 min in PBS.

For the immunoperoxidase localization of GAD or PV, sections were processed through a 1:400 dilution of biotinylated goat anti-rabbit IgG (Vector, 30 min), ABC (1:200; Vector) for 30 min, 3′-diaminobenzidine (DAB; Sigma), and H_2O_2 in 0.1 M TBS for 6 min. All incubations were separated by washes in TBS.

Sections were then fixed for 1 h in 2% osmium tetroxide (TAAB Lab, Aldermaston, Berkshire, UK) and dehydrated using increasing concentrations of ethanol and propylene oxide. Sections were applied to slides pretreated with Liquid Release and flat-embedded in Epon 812 (TAAB). Ultrathin sections (70–72 nm thick) through the rostral part of the RSC (AP −2.1 to −3.8 from bregma; Paxinos and Watson, 1998) were obtained using a Leica UCT ultratome. Sections were contrasted with 1% lead citrate on formvar-coated single-slot grids. Finally, the preparations were analyzed with a JEOL 1200 EX-II transmission–electron microscope, equipped with an Advanced Microscopy Technique digital camera. Figures were assembled and adjusted for brightness and contrast in Adobe Photoshop.

Data analysis

For quantitative analysis, tissue sections from rats with good preservation of ultrastructural morphology and with both markers clearly apparent were used.

At least 10 grids containing five to 10 ultrathin sections each were collected from a minimum of three plastic-embedded sections from each rat. All profiles containing immunoperoxidase labeling and immunogold labeling in the same fields of at least 11,000 magnifications were

photographed and later classified. Selective immunogold-labeled profiles were identified by the presence, in single thin sections, of at least three times the number of immunogold particles within a cellular compartment than in adjacent compartments.

RESULTS

The basal forebrain cholinergic fiber pathway region in the RSG

Three rats were successfully injected with the anterograde tracer PHA-L into the HDBm. The PHA-L labeled fibers and terminals were found to be most dense in a small zone just below the packed cell layers II/III and spread out in layer Ia (Fig. 1A).

The pattern of cholinergic axons (dense terminals throughout layer Ia, and a small zone just below the packed cell layers II/III), as detected by ChAT, vAChT, p75, and CHT immunoreactivity (Fig. 1B1–B5), was the same as the labeling pattern of axon terminals in layers I–IV of the RSG, following PHA-L injection into the basal forebrain (Fig. 1B1–B5). Layer V contained a moderately dense collection of predominantly radially running fibers (Fig. 1B2–B4).

Distribution of α7nAChR-immunoreactive cells and Alexa fluor 488-αBTX-labeled cells in the RSG

To confirm the specificity of α7nAChR immunolabeling, we performed two independent tests: (1) evaluation of labeling with a monoclonal antibody raised against a larger epitope of the α7 subunit (M220 monoclonal: amino acids 380–400), using both light and electron microscopy. Under light microscopy, immunolabeling of the RSG revealed diffuse α7nAChR immunoreactivity (α7nAChR-ir) throughout the cell bodies and cell processes of individual principal neurons (Fig. 2A2, C2). The most intense α7nAChR-ir was observed in layers II/III. The cortical layer location of many α7nAChR labeled cells was consistent with their identity as RSG cortical neurons. It was not possible to obtain accurate numbers of α7nAChR-immunoreactive neurons in layers II/III of the RSG due to the presence of diffuse α7nAChR labeling within the principal neurons. The density of α7nAChR-positive neurons in layers IV/V was lower than that in layers II/III (Fig. 2A2, C2). There were scattered interneurons containing α7nACh-ir in layer I (Fig. 2A2). α7nAChR-positive puncta in layer I were sometimes evident in thick straight processes, presumed to be dendritic bundles that emitted from the somata (Fig. 2C2, arrowheads). Omission of the primary antibody resulted in the complete loss of α7nAChR labeling in the RSG (data not shown). (2) We performed labeling for αBTX. The density of neurons labeled with αBTX was lower than that of α7nACh-immunoreactive neurons (Fig. 3A1–E1). αBTX-positive neurons were found primarily in layers II/III, and sparsely scattered near layers IV/V. Interneurons in layer I of the RSG also contained α-BTX-binding sites (Fig. 3A1, B1). αBTX-binding sites in layers I–III of the RSG were also observed in thick straight processes presumed to be dendrites, that emitted from the somata (Fig. 3A1, B1, C1, and E1). αBTX binding neuropiles also formed bundles in layer I (Fig. 3D1).

Dual immunolabeling with antisera against the α7nAChR and GAD or PV

To confirm the GABAergic nature of neurons expressing high levels of α7nAChR, we determined the degree of cellular co-localization of α7nAChR-ir with GAD-ir or PV-ir. α7nAChR-ir was observed in subsets of GABAergic neurons (either GAD- or PV-immunoreactive cells) in layers I–III of the RSG (Fig. 2A3, B3, B6, C3, and D3). As shown in Fig. 2 (A3, C3), α7nAChR-ir, GAD-ir, and PV-ir exhibited largely similar distribution patterns in layers II/III of the RSG. The α7nAChR-immunolabeled neurons in layer I also expressed GAD-ir (Fig. 2A3, B3). Double immunolabeling for α7nAChR and PV revealed that the density of α7nAChR-immunolabeling corresponds to the PV-immunolabeled dendritic bundles in layer I (Fig. 2C1–C3). Analysis of the percentage of cellular co-expression of α7nAChR-ir and GAD-ir in layer-III of the RSG indicated that more than 97% of GAD-immunoreactive interneurons and 92% of PV-immunoreactive interneurons contain α7nAChR-ir (Table 1).

Co-expression of αBTX binding sites and GAD-ir or PV-ir in RSG interneurons

Immunocytochemistry and Alexa488-αBTX binding in the same section were employed in order to determine whether αBTX-binding sites colocalize with GAD-ir or PV-ir. Confocal microscopy revealed the co-expression of αBTX binding sites and GAD-ir or PV-ir in several layers of the RSG (Fig. 3A3–E3). In layers II/III, most αBTX-labeled cells also expressed GAD-ir or PV-ir (Fig. 3C3, E3: arrows). Some of the αBTX-labeled neurons in layers II/IV were PV- or GAD-negative (Fig. 3C3, E3: arrowheads). Quantitative analysis demonstrated a very high degree of cellular co-expression of αBTX-binding sites and GAD-ir/PV-ir in the RSG (Table 1). Within the population of interneurons expressing αBTX in the RSG, 100% contained GAD-ir in layer I and in layers II/III, 92% contained GAD-ir, and 84% contained PV-ir. The degree of co-expression of αBTX-binding sites and GAD-ir or PV-ir may have been underestimated because αBTX-binding sites (corresponding to the α7nAChR signal) are confined to the surface of the section, but GAD- or PV-immunoreactive neurons can be seen throughout the depth of the section.

The interneurons expressing αBTX-binding sites in layer I also express 5HT3a that label for GAD-ir

As previously reported (Lee et al., 2010; Miyoshi et al., 2010), the largest group of superficial neocortical GABAergic interneurons express the glycoprotein reelin which is a member of the serotonin family (5HT3a) containing the 5HT3a group (Rudy et al., 2011).

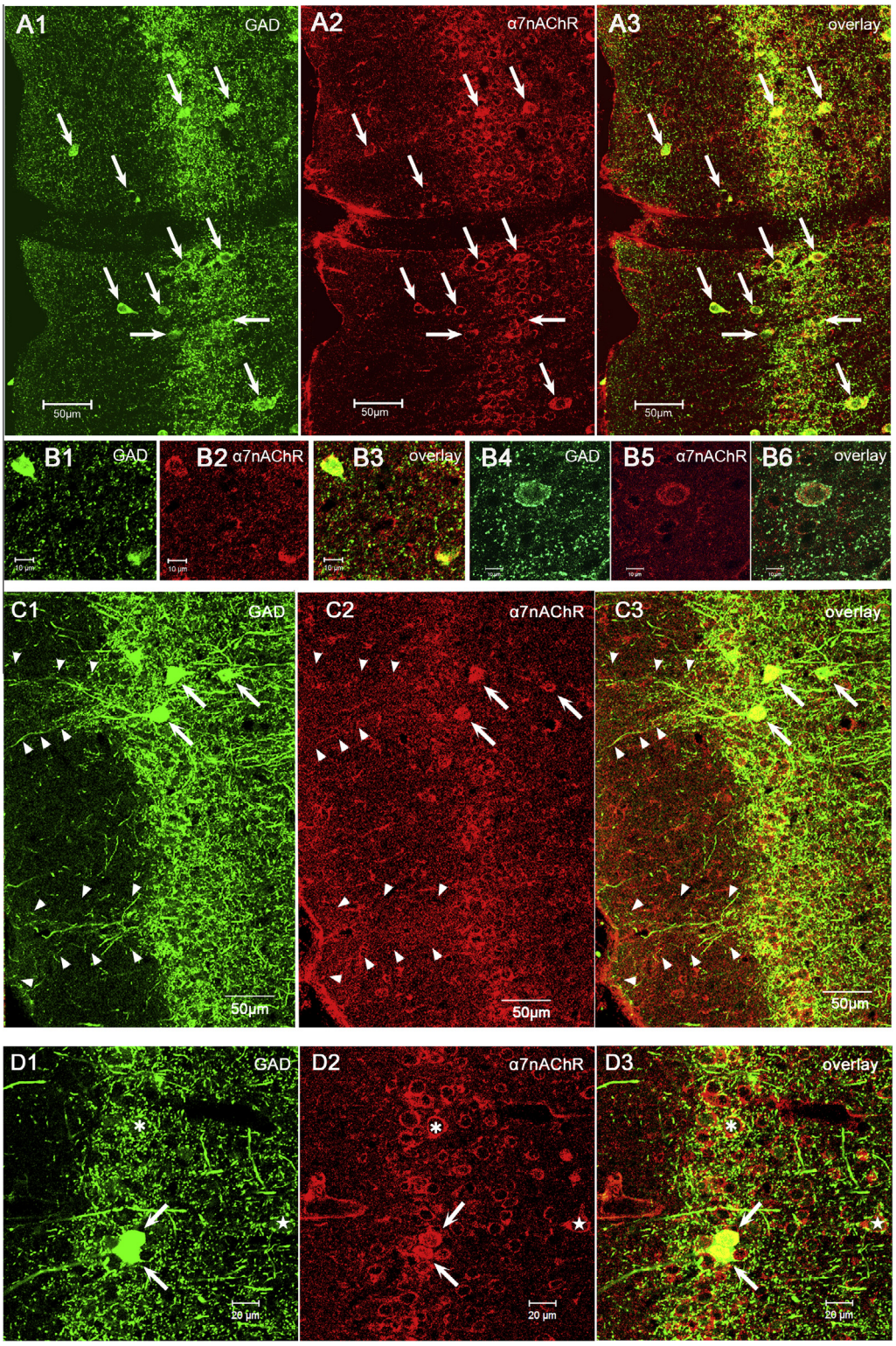

Fig. 2. Confocal microscopic images for α7nAChR-immunoreactivity (α7nAChR-ir) in GABAergic neurons in layer I–III of the RSG. (A, B) α7nAChR/GAD double-immunostained sections. (C, D) α7nAChR/PV double-immunostained sections. α7nAChR was visualized using Cy3-conjugated secondary antibody (A2, B2, C2, D2: red) for Cy2-labeled GAD or PV colocalization (A1, B1, C1, D1: green). Overlaid images show the region of colocalization (A3, B3, C3, and D3). (A1–A3) Arrows point to α7nAChR/GAD double-immunolabeled neurons in layer I–III. (B1–B3) In layer I, the soma of a α7nAChR/GAD double-labeled neuron. (B4–B6) The somata of α7nAChR/GAD double-labeled in layer II/III. (C1–C3) α7nAChR-immunoreactivity co-expressed with PV-labeling, particularly in layer II/III (arrows). α7nAChR-ir neurons in layer I do not express PV-immunoreactivity. α7nAChR immunolabeled grains in layer I converge on PV-labeled dendritic bundles (C1–C3, arrowheads). (D1–D3) Arrows point to α7nAChR/PV double-labeled neurons in layer II/III. PV-positive boutons surround α7nAChR-expressing somatodenrites (∗, ★), which are negative for PV. (For interpretation of the references to color in this figure legend, the reader is referred to the web version of this article.)

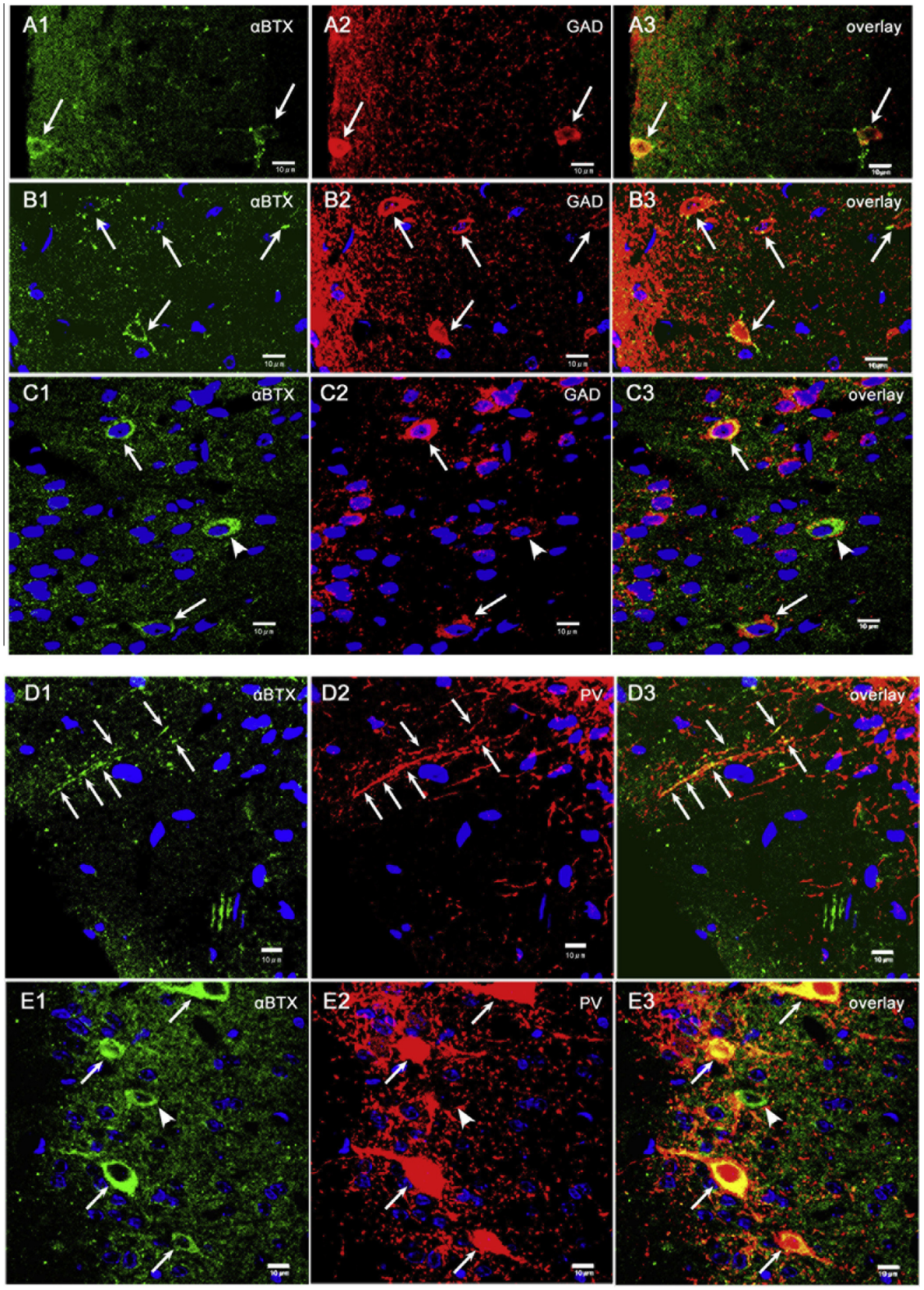

Fig. 3. Confocal microscopic images showing αBTX-binding sites on GABAergic neurons in layer I–III of the RSG. (A1–A3, B1–B3, C1–C3) Immunofluorescence of GAD labeling, followed by Alexa488-αBTX labeling. (D1–D3, E1–E3) Immunofluorescence of PV labeling, followed by Alexa488-αBTX labeling. (A, B) Double-labeling for αBTX and GAD-immunoreactivity (-ir) show αBTX/GAD labeled neurons in layer I (arrows). (C) Double-labeling for αBTX and GAD-ir or PV-ir show αBTX/GAD-labeled neurons in layer II/III (arrows). (D) αBTX binding sites are associated with PV-labeled dendritic bundles in layer I. Notably, not all neurons expressing αBTX-binding sites also express PV-ir dendritic bundles (arrows). (E) αBTX-binding sites are frequently present on PV-labeled cells (arrows) and neuropiles (dendrites and axon terminals) in layer II/III. (C, E) Some αBTX-binding site-expressing neurons in layer II/III are GAD- or PV-negative (arrowheads).

Table 1. Presence of α7nAChR/αBTX in GAD-, PV-, and reelin-immunoreactive cell bodies. The total number of α7nAChR-expressing neurons was counted in 21 sections from three different rats

Location	α7nAChR + /GAD +	αBTX + /GAD +	Reelin + /αBTX +	α7nAChR/PV +	αBTX + PV +
Layer I	100% (n = 60)	100% (n = 31)	83% (n = 29)		
Layer II/III	97% (n = 93)	92% (n = 45)		98% (n = 91)	84% (n = 57)
	n = GAD +	n = αBTX +	n = αBTX +	n = PV +	n = αBTX +

To determine the identity of interneurons expressing αBTX-binding sites in layer I of the RSG, the immunocytochemical characteristics of GABAergic subpopulations were compared with the localization of αBTX-binding sites in the same sections. A subpopulation of neurons in layer I was reactive to an antibody to reelin (an extracellular matrix protein), and was labeled by αBTX (Fig. 4A1–A3, B1–B3). Images were obtained with confocal microscopy and processed for 3D rendering and rotation to evaluate the potential cellular location of labeled binding sites (Fig. 4C1–C5, D1–D5, and E1–E5). Despite a low density of GAD-immunoreactive neurons in layer I of the RSG, αBTX-binding sites were expressed on GAD-reactive soma and dendrites (Fig. 4C1–C5, D1–D5, E1–E5). These results provide morphological evidence that α7nAChR

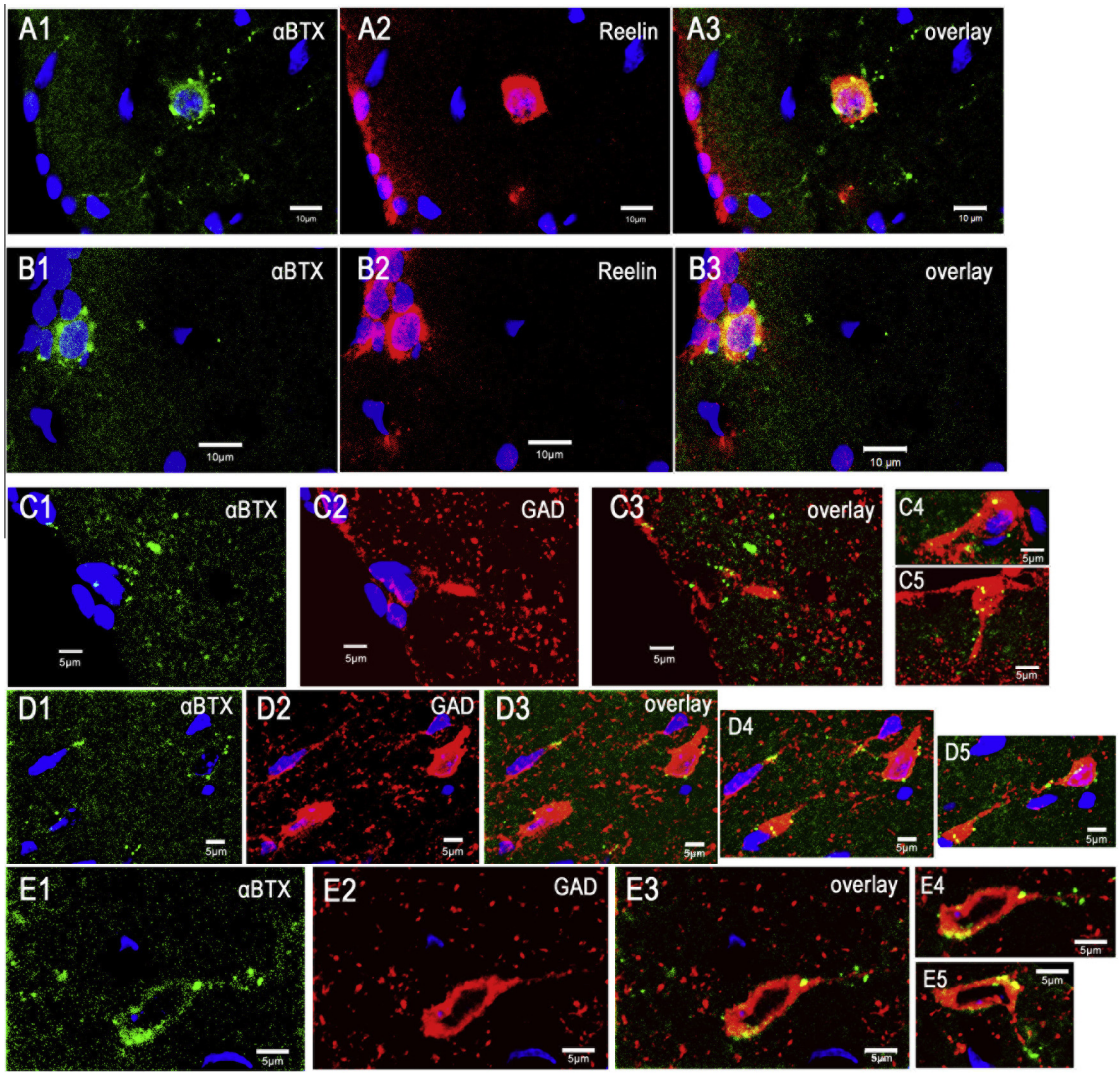

Fig. 4. Coexpression of αBTX-binding sites and reelin or GAD in layer I of the RSG. (A, B) Confocal images show αBTX-binding sites (A1, B1, green, Alexa488) on reelin-immunoreactive neurons in layer I (A2, B2, red, and Cy3). Overlays in A3 and B3 demonstrate that reelin-immunoreactivity is expressed by Alexa 488-αBTX–labeled GABAergic neurons in layer I. (B) αBTX/reelin double-labeled neurons were located just under the pia. (C1–C3, D1–D3, E1–E3) Double-labeling for αBTX/GAD shows αBTX-binding sites on four GABAergic neurons. (C) As shown in (B), αBTX-binding sites are located on a GABAergic neuron located just under the pia. (C4–C5, D4–D5, and E4–E5) αBTX binding sites enriched in GAD-labeled somatodendrites in layer I (as 3-D rendered and rotated views, C3, D3, and E3). (For interpretation of the references to color in this figure legend, the reader is referred to the web version of this article.)

may mediate the activation of layer I reelin-/GAD-immunoreactive interneurons.

Neurons expressing αBTX-binding sites in layers II/III receive GABAergic terminals

As shown in Fig. 5A, B, neurons expressing αBTX binding sites that did not contain GAD-ir or PV-ir (Fig. 5A2, B2), showed multiple contacts with GAD- or PV-immunoreactive boutons (arrows) on their somatodendrites in layers II/III of the RSG. These GAD- or PV-negative, αBTX-positive neurons are consistent with previous reports demonstrating that [125I] α-BTX/α7nAChR-mRNA are frequently co-expressed within a subset of GABAergic interneurons (Freedman et al., 1993; Morales et al., 2008).

In order to determine the relative density of αBTX binding sites in the RSG (Fig. 5A3, B3), we also evaluated a sample of the hippocampal CA1 region containing a high density of GABAergic axons. In the hippocampal CA1 field (Fig. 5C, D), the stratum oriens demonstrated a high density of αBTX-positive interneurons and neuropiles. αBTX-positive somatodendrites strongly contacted with GAD-ir/αBTX or PV-ir/αBTX double-labeled terminals (Fig. 5C3, D3: arrows).

Electron microscopy demonstrates that α7nAChR is present in the cell bodies and neuropiles of GAD- or PV-positive neurons

Subcellular localization of α7nAChR in GABAergic neurons in layers I–III of the RSG

To investigate whether the α7nAChR-ir includes GABAergic soma and neuropiles, we performed double labeling for GABAergic markers (GAD and PV) and α7nAChR. α7AChR-ir was identified using silver-enhanced immunogold (α7AChR-ig); GAD- or PV-ir was identified by a DAB reaction product (GAD-/PV-ip). Consistent with the confocal microscopy data, dual-labeled electron microscopy revealed that α7nAChR-ig was located in the cytoplasm of the soma and neuropiles in a subpopulation of GAD-ip or PV-ip labeled neurons in layers I–III of the RSG (Fig. 6A, B, E, and F). GAD- or PV-ip labeled axon terminals containing α7nAChR-ig formed synapses with α7nAChR/GAD or α7nAChR/PV dual-labeled somatodendrites (Fig. 6B, E1–E2, F1). In some instances, α7nAChR and GAD double-labeled axons formed synaptic contacts with non-GAD labeled somata containing α7nAChR-ig (Fig. 6C: arrow), and apposed α7nAChR-ig single-labeled neurons (Fig. 6D1, D2). α7nAChR-ig was predominantly localized in the perinuclear cytoplasm, where the immunogold particles were associated with Golgi lamella (Fig. 6C).

To investigate whether GABAergic neuropiles within layer I express α7 nAChRs, sections were co-labeled with antibodies to GAD and PV. α7nAChR-ig was observed both in the cytoplasm and on the surface membrane of GAD-/PV-ir neuropiles containing axon terminals and dendrites (Fig. 7A, B). Dual-labeled axon terminals containing α7nAChR-ig and GAD-ip or PV-ip apposed non-labeled dendrites and spines (Fig. 7A1, A2, B1, B2: arrowheads). The α7nAChR and GAD double-labeled axon terminals formed symmetrical synapses on dendrites containing α7nAChR-ig (Fig. 7A1, A2: arrows). Together, these observations provide strong evidence that α7nAChR is primarily located on GABAergic neurons in layers I–III of the RSG. In layer I, GAD- or PV-labeled small dendrites containing α7nAChR-ig made asymmetric synapses with unlabeled axon terminals (ut) (Fig. 7A, B3: arrows).

DISCUSSION

The present study was performed in order to characterize the CBF projections from the MS–DB to layers of the RSG using anterograde neural tracing (PHA-L) and immunohistochemical detection of several cholinergic markers, such as ChAT, vAChT, CHT and p75. In addition, we tested the hypothesis that α7nAChRs reside on GABAergic interneurons in the basal forebrain cholinergic terminal fields of the adult rat RSG. Here, we demonstrate that the basal forebrain cholinergic terminal fields on RSG are associated with an area that expresses α7nAChR and that α7nAChRs are expressed on GABAergic cells in layer I and PV-immunopositive cells in layers II/III of the rat RSG.

CBF terminal fields in the RSG are associated with α7nAChR expression

CBF terminal field. Our results using the anterograde tracer PHA-L revealed that PHA-L-labeled projection fibers from the BF are frequently observed in layer Ia, as well as layers II/III of the RSG. Our results using antibodies against a variety of cholinergic markers (CHT, ChAT, vAChT, and p75NTR) showed a similar pattern to acetylcholinesterase staining (Slomianka and Geneser, 1991; Tengelsen et al., 1992; Gage et al., 1994) and to the ChAT/vAChT immunostaining results provided by previous studies (Eckenstein et al., 1988; Lysakowski et al., 1989; Gilmor et al., 1996; Schafer et al., 1998). With regard to projection fibers to the RSG, several studies have reported that these fibers are mainly derived from the HDBm (Rye et al., 1984; Senut et al., 1989; Gonzalo-Ruiz and Morte, 2000). In addition, injection of various anterograde tracers (3H-amino acids, PHA-L, and DiI) into the HDBm has shown that the labeled projection fibers are densely distributed in layers II/III of the RSG (Saper, 1984; Gaykema et al., 1990; Robertson et al., 2009). Recently, it was shown that after the damage of BFC neurons with 192-IgG immunotoxin, which is specific for cholinergic neurons in the basal forebrain (Heckers et al., 1994), the PHA-L labeling of fibers layer I and layers III/V of the RSG is lost (Murakami et al., 2000). Therefore, layers Ia and II/III of the RSG are likely to be target regions affected by ACh derived from cholinergic projections from the BF.

α7nAChR expression in layers I–III of the RSG. It should be noted, however, that we need to be careful in interpreting results when using several commercially

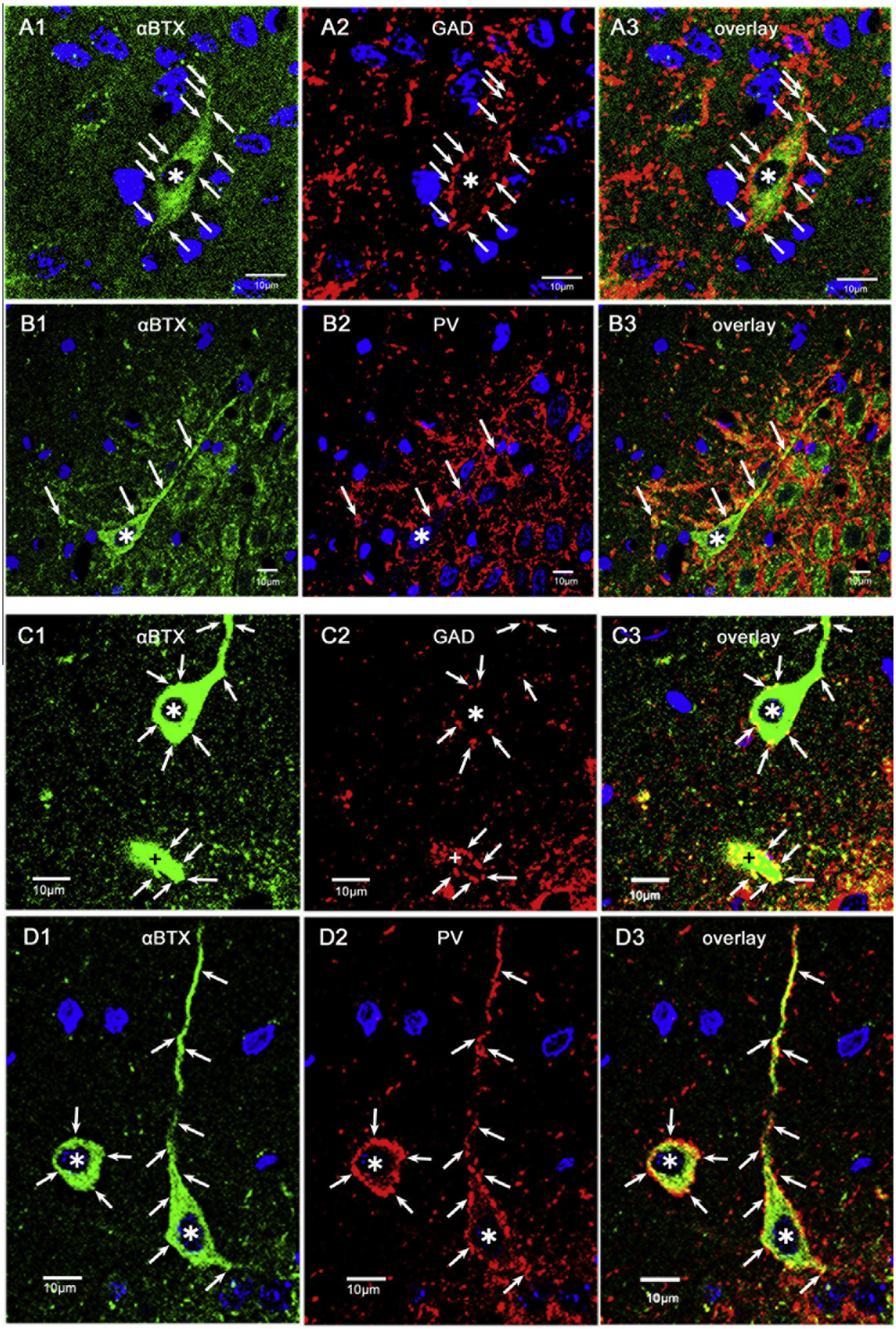

Fig. 5. Confocal images of double fluorescence labeling of αBTX/GAD or αBTX/PV in layer II/III of the RSG and in the hippocampal CA1 stratum oriens. (A, B) αBTX-binding site-expressing interneurons (A1, B1, ∗) that do not contain GAD (A2, ∗) or PV immunoreactivity (B2, ∗), showed multiple contacts with GAD- or PV-labeled boutons on their somatodendritic regions in layer II/III of the RSG (arrows). (C, D) Note that GAD- or PV-negative, but αBTX-positive interneurons (∗) were innervated by GAD- or PV-labeled boutons in the CA1 region of the hippocampus. A high density of αBTX-expressing interneurons (C, D: ∗) and somatodendrites (C: +) in the stratum oriens of the CA1 subfield proved to be GAD- or PV-negative. As shown in (A, B), αBTX-binding site-expressing somatodendrites strongly contact with GAD-ir or PV labeled terminals (arrow).

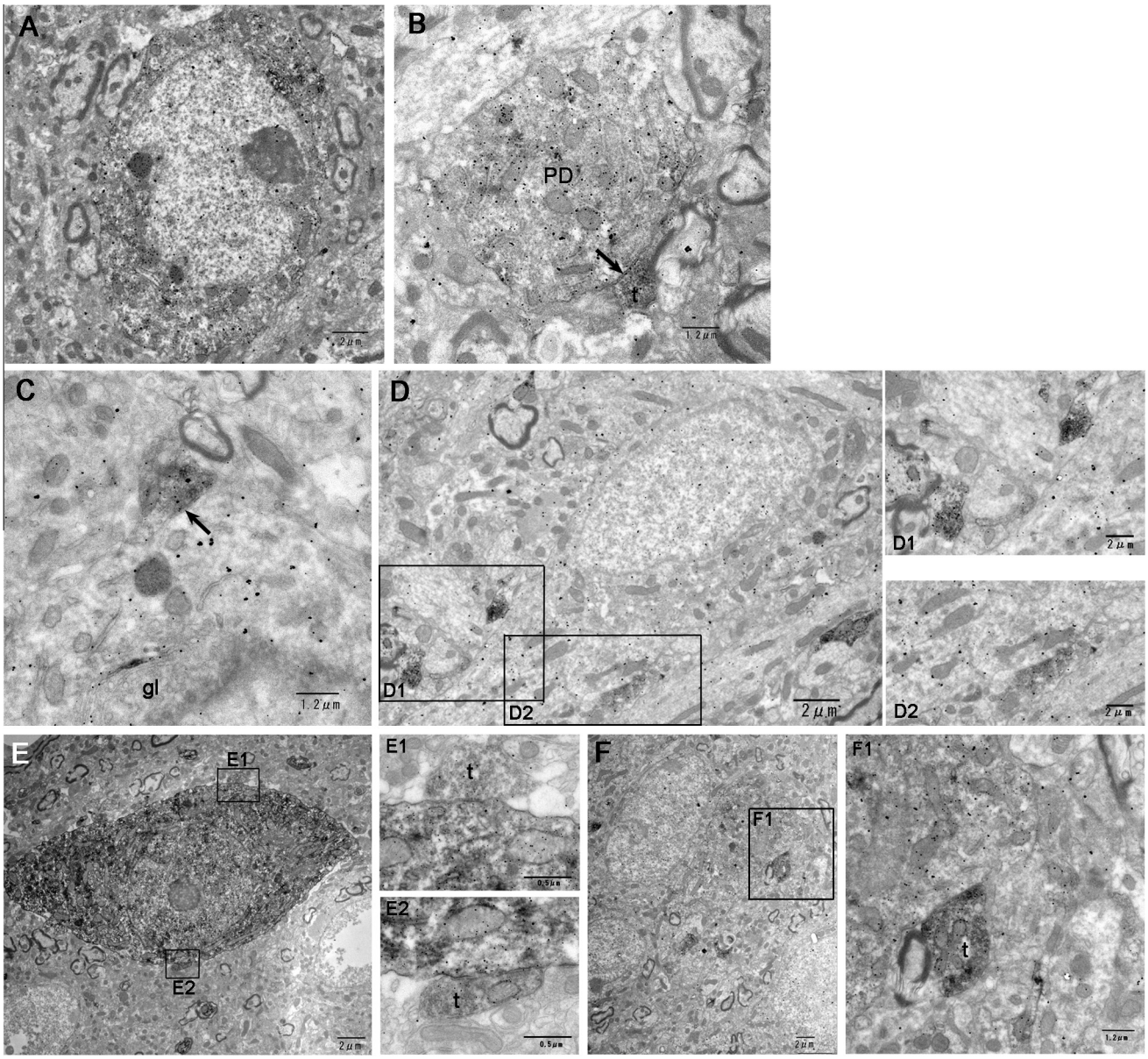

Fig. 6. Electron microscopic images showing the subcellular localization of α7nAChR in GABAergic and non-GABAergic neurons in layer II/III of the RSG. (A) α7nAChR-ig is found in GAD-ip soma in layer I. (B) α7nAChR/GAD-labeled proximal dendrite (PD) receives synaptic contacts from a terminal (t) containing α7nAChR-ig/GAD-ip (arrow) in layer I. (C) α7nAChR/GAD-labeled terminal (t) makes a symmetrical synapse with a soma containing α7nAChR-ig (arrow). α7nAChR-ig has a prominent location in the perinuclear cytoplasm, where the immunogold particles are associated with the outer Golgi lamella (gl). (D) GAD-negative soma with α7nAChR-ig labeling apposes two terminals containing α7nAChR-ig/GAD-ip in layer II/III of the RSG. Boxed regions are shown at higher magnification in insets D1 and D2. (E, F) α7nAChR/PV-labeled somata receive synaptic contact from terminals containing α7nAChR-ig/PV-ip in layer II/III. In insets E1, E2, F1: α7nAChR/PV labeled terminals (t) form symmetric synapses (arrows) on double-labeled soma (boxed regions, shown at higher magnification).

available antibodies to α7nAChR, because subsequent studies which used the intrahippocampal injection of lipopolysaccharide (LPS) into α7nAChR-knockout mice revealed that the α7nAChR immunolabeling was nonspecific (Herber et al., 2004; Jones and Wonnacott, 2005). For this reason, we used Alexa-488-conjugated αBTX to verify the results of our α7nAChR immunostaining. However, when quantitatively analyzing the binding sites of αBTX, it is necessary to underestimate the number of neurons positive for αBTX, an antagonist at α7nAChRs. This is because α7nAChR undergoes desensitization followed by rapid activation of the calcium channel (Alkondon et al., 1992; Castro and Albuquerque, 1995; Gray et al., 1996), and the runoff of ACh is reduced due to the inactivation of BF cholinergic neurons in anesthetized animals (Platt and Riedel, 2011).

The present findings reveal that cells strongly expressing α7nAChR are found in layers I and II/III of the RSG. As shown in Table 1, in layers I–III of the RSG, the number of cells expressing αBTX-binding sites was much less than the number of cells stained by α7nAChR, but similar to the distribution of cells stained

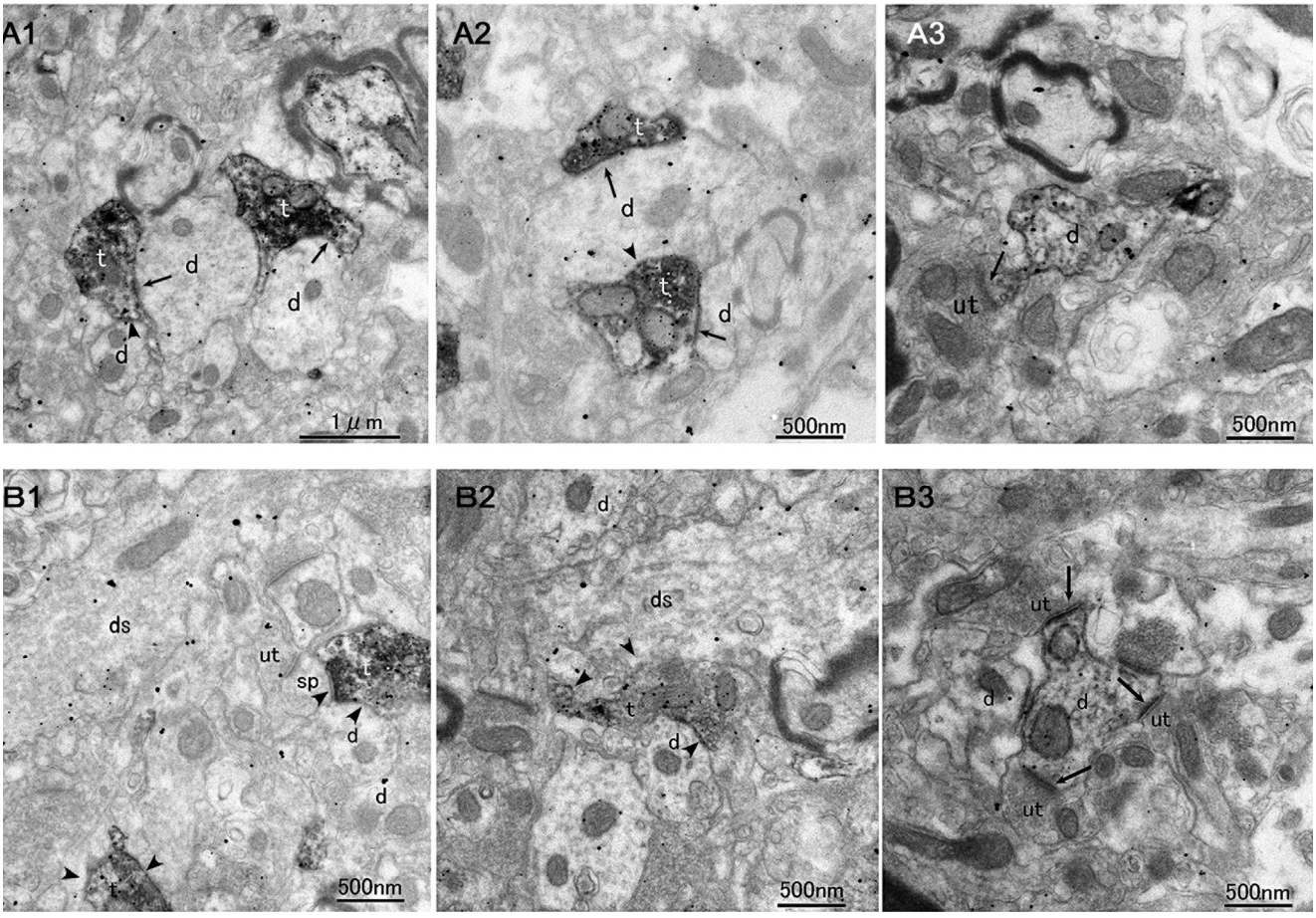

Fig. 7. Electron microscope images showing the localization of α7nAChR in GABAergic neuropiles in the RSG layer I. (A1–A3) Double-labeling for α7nAChR-ig and GAD-ip. Two axonal terminals labeled for both α7nAChR-ig and GAD-ip contact (arrows) small dendrites labeled for α7nAChR (B1, B2). In B3, the unlabeled axon terminal (ut) is apposed to a small dendrite double-labeled for α7nAChR-ig and GAD-ip (arrow). (B1–B3) Double-labeling for α7nAChR-ig and PV-ip. (B1, B2) PV-negative dendritic shaft (ds) contains labeling for α7nAChR-ig. Double-labeled axon terminals (t) for α7nAChR-ig and PV-ip appose to unlabeled spines or dendrites (arrowheads). In B3, three unlabeled axon terminals (ut) form asymmetric synapses on a PV-labeled small dendrite containing α7nAChR-ig (arrows).

by α7nAChR. These findings show that the distribution of α7nAChR-immunolabeled cells also corresponds to the localization of cortical principal cells. In a study using the same antibody to α7nAChR, α7nAChR expression in the frontal cortex exhibited similar results to those of the present study (Duffy et al., 2009). In particular, in layer I of the RSG, αBTX-binding cells as well as α7nAChR-immunoreactive cells were present. Additionally, αBTX-binding neuropiles were dense in layer Ia, where cholinergic and thalamic terminals are concentrated. This means that the majority of αBTX-binding sites are localized within the compartment containing the cell bodies and neuropiles. The findings regarding αBTX-binding sites in the RSG have not been observed at the cellular level, while strong expression of 125I-αBTX has been demonstrated only in layer I of the monkey RSG (Han et al., 2003).

α7nAChR expression in the hipocampal region. Within the same section, strong αBTX expression and immunostaining of α7nAChR were observed not only in the CA1–CA3 pyramidal cell layer of the hippocampus, but also in cells of the granular layer of the dentate gyrus (data not shown), where cholinergic fibers converge (Dougherty and Milner, 1999). These results are consonant with those of previous reports; autoradiography of 125I-αBTX-binding (Freedman et al., 1993; Frazier et al., 1998b; Adams et al., 2001), *in situ* hybridization of α7nAChR mRNA expression (Morales et al., 2008; Son and Winzer-Serhan, 2008) and α7nAChR immunostaining (Fabian-Fine et al., 2001). Therefore, these findings strongly support the notion that CBF terminal fields in the RSG and hippocampus are associated with α7nAChR expressing areas.

α7nAChRs are present on GABAergic interneurons in the RSG

At the light microscopical level, our results indicate that more than 99% of PV-ir and GAD-ir cells in layers I–III of the RSG are strongly immunolabeled for α7nACR, and that all of the GAD-ir cells distributed in layer I are also α7nAChR immunopositive. The present findings that αBTX-binding site expression is particularly localized to GABAergic cells support the results of our

α7nAChR immunostaining. In other words, our data indicate that αBTX-binding site expression is present not only in all GAD-positive cells of layer I, but also in all of the GAD-positive and PV-positive cells of layers II–IV. In addition, we confirmed that αBTX-binding sites are expressed in GAD-negative or PV-negative multipolar cells, which appear to be non-pyramidal cells in layers II/III. Our electron microscopy findings from double immunostaining using GAD or PV and the α7nAChR antibody are summarized below:

(1) GAD-positive somatodendrites labeled with DAB in layer I of the RSG were also gold labeled for α7nAChR.
(2) DAB-labeled PV-positive soma and dendrites coexist in layers II/III.

These findings strongly suggest that α7nAChR expression is localized in the GABAergic interneurons of layer I, PV-positive GABAergic interneurons of layers II/III, and other types of GABAergic interneurons. To date, a great deal of attention has been paid to the localization of nAChRs in the hippocampal cortex, because this area receives a large number of cholinergic afferents from the basal forebrain. In the hippocampal regions receiving cholinergic projections, 125I-αBTX autoradiography reveals that α7nAChR is expressed in both GABA- and cholecystokinin-positive cells distributed from the pyramidal cell layer of CA1 to the plexiform layer and in somatostatin-positive cells of the oriens layer of the hippocampus (Jones and Yakel, 1997; Frazier et al., 1998b). *In situ* hybridization studies of α7nAChR mRNA provide evidence that 94% or more cells expressing GAD mRNA, which are distributed between the plexiform layer and oriens layer of the hippocampus, also express α7nAChR mRNA and that more than half of the cholecystokinin-positive cells also express α7nAChR mRNA (Frazier et al., 1998b). Additionally, there is electrophysiological evidence that nAChRs are abundant on the somata of interneurons in the CA1 region of the hippocampus (Jones and Yakel, 1997; Frazier et al., 1998a). These findings indicate that α7nAChR is localized on GABAergic interneurons of the rat RSG, as well as in the hippocampal cortex.

The coexistence of PV-positive neuropiles (dendrites and axons) and α7nAChRs

In the rat RSG, using αBTX labeling following α7nAChR immunostaining, we confirmed that αBTX-labeled cells are colocalized with PV-positive cells. Additionally, the present study found α7nAChR expression on the column-like bundles of PV-ir dendrites in layer I of the RGS. PV-positive neurons have been reported to form the neuropiles in layer I of the RSG (Ichinohe and Rockland, 2002). This suggests that PV-ir interneurons of layers II/III may be influenced by ACh. While it has been identified that PV-positive interneurons express α7nAChR in the human brain (Krenz et al., 2001), and the rat ventral medulla (Dehkordi et al., 2007), this is the first time that this has been confirmed in the rat RSG. PV-positive cells in a group of cortical interneurons belong to the fast-spiking (FS) cell group (Kawaguchi and Kondo, 2002). These PV-positive FS cells in layers II/III of the rat sensory cortex are not directly excited by the administration of ACh (Gulledge and Kawaguchi, 2007; Letzkus et al., 2011). In contrast, PV-positive FS cells of the hippocampal CA3 are activated via cholinergic receptors (Gulyás et al., 2010), and FS cells in layers II/III of the forebrain are excited by α7nAChRs (Poorthuis et al., 2013). This strongly suggests that PV-positive neurons distributed in the RSG are directly affected through α7nAChR.

The present study provides direct neuroanatomical evidence for the expression of α7nAChRs on both somatodendritic and neuronal elements within PV-stained neurons in layers I–III of the RSG.

Evidence that interneurons expressing αBTX-binding sites in layer I are a group of 5HT3a expressing GAD-ir

Recent embryological data provide evidence that GABAergic cortical interneurons are embryonically derived from medial or caudal ganglionic eminences, and that almost 100% of neocortical interneurons (Lee et al., 2010) express PV, somatostatin, or 5HT3a (Rudy et al., 2011). Rudy et al. (2011) reported that the majority of GABAergic interneurons in isocortex layer I in rodents occupy the group 5HT3a (Rudy et al., 2011), and that interneurons in layer I of the adult rat neocortex express reelin (a large extracellular matrix glycoprotein) (Ramos-Moreno et al., 2006).

The present study revealed that the reelin-positive GABAergic interneurons localized in layer I of the RSG express αBTX-binding sites. Our electron microscopy findings also show that GAD-positive somatodendrites labeled with DAB in layer I of the RSG coexpress α7nAChR (shown by immunogold labeling). This suggests that GABAergic interneurons of layer I of the rat RSG may be influenced via α7nAChR when ACh is released from cholinergic projections between the BF and RSG.

Recent *in vivo* experiments suggest that GABAergic interneurons in layer I of the rat auditory cortex may disinhibit interneurons in layers II/III via the activation of nAChR by ACh released from BF projections (Letzkus et al., 2011). Suppressive interneurons in layer I related to this local circuit, and PV-positive interneurons in layers II/III of the rat RSG were inhibited by methyllycaconitine, a α7nAChR inhibitor (Christophe et al., 2002; Letzkus et al., 2011). We provide morphological evidence supporting these *in vivo* experimental results that α7nAChR is localized to suppressive interneurons distributed in layer I and layers II/III of the rat RSG.

The non-GAD-/non-PV-immunoreactive neurons expressing αBTX-binding sites in layers II/III receive GABAergic terminals

In layers II/III of the rat RSG, multiple contacts of GAD-immunoreactive or PV-immunoreactive terminals were confirmed on large multipolar neurons expressing

GAD-immunoreactive or non-PV-immunoreactive αBTX-binding sites. In a polymorphic cell layer in the CA1 hippocampal region of the same brain section, the same findings were confirmed. 125I-αBTX autoradiography has also confirmed that the multiform layer of the hippocampus expresses αBTX-binding sites in PV-, CCK-, or VIP-immunoreactive cells (Freedman et al., 1993; Frazier et al., 1998b; Buhler and Dunwiddie, 2001; Morales et al., 2008). Because the present study did not use markers for CCK/VIP-positive GABAergic cell populations, it could not be confirmed whether the large multipolar neurons expressing αBTX-binding sites were in fact GABAergic neurons. However, considering that αBTX-expressing sites do not exist in pyramidal cells, and that cells expressing αBTX-binding sites are large multipolar neurons, it is suggested that the large multipolar neurons may be GABAergic.

GABAergic innervation in relation to α7nAChRs

In this study, our electron microscopy data indicated that α7nAChR is localized in the cell bodies, dendrites, and axon terminals of PV-positive and GAD-positive cells. These results are in agreement with those of a previous study using α7nAChR-immunohistochemical electron microscopy (Fabian-Fine et al., 2001). In cultured hippocampal inhibitory neurons, the coexistence of post-synaptic GABA-A receptors and αBTX-binding sites was confirmed on the dendrites of GABAergic cells (Kawai et al., 2002). One issue to consider in the ultrastructural observation of α7nAChR localization is α7nAChR reliability and the inhibition of α7nAChR antibody staining by aldehyde fixation (Jones and Wonnacott, 2004). The α7nAChR antibody used in the present study has been previously applied in both electron and fluorescence microscopy (Dominguez del Toro et al., 1994; Fabian-Fine et al., 2001; Levy and Aoki, 2002; Centeno et al., 2006) and assayed in western blotting of the cerebral cortex (Duffy et al., 2009). Duffy et al. (2009) observed α7nAChR localized in the dendrites, dendritic spines, and cytoplasm of the cell bodies of pyramidal cells in the prefrontal cortex using the pre-embedding method with fixed sample.

Our electron microscopy findings provide evidence that GAD-positive cells expressing α7nAChR in layer I, or PV-positive cells in layers II/III receive synaptic connections from GABAergic axon terminals expressing α7nAChR. This suggests that both GAD- and PV-positive cells are intrinsically or externally regulated by GABAergic neurons in the RSG (Christophe et al., 2002; Miyashita and Rockland, 2007). There is immunocytochemical evidence that α7nAChR is present at postsynaptic sites of glutamatergic synapses in the hippocampus and neocortex, along with electrophysiological evidence of postsynaptic nicotinic currents in the neocortex and hippocampus. However, morphological data shows that GABAergic and glutamatergic synapses in the stratum radiatum of the CA1 area have α7nAChRs. These electron microscopic data were obtained using a post-embedding method (Fabian-Fine et al., 2001). Furthermore, in the ventral tegmental area, α7nAChR expression has been examined with both the pre- and post-embedding methods, using biotinylated αBTX. The results showed that α7nAChRs are primarily localized in the cytoplasm of the presynaptic region in different populations of dopaminergic and non-dopaminergic neuronal terminals, often in the extrasynaptic area as well as the perisynaptic area (Jones and Wonnacott, 2004). These findings suggest that both GAD- and PV-positive cells receive intrinsic or external regulations of GABAergic neurons in the RSG (Christophe et al., 2002; Miyashita and Rockland, 2007). However, depending on the interneurons involved, α7nAChR activation can lead to either inhibition or disinhibition of RSG principal neurons and can have divergent effects on synaptic plasticity (Fujii et al., 2000; Ji and Dani, 2000; Alkondon and Albuquerque, 2001; Buhler and Dunwiddie, 2001, 2002; Ji et al., 2001).

In summary, this study provides direct neuroanatomical evidence for the expression of α7nAChRs on a subset of GABAergic interneurons in layers I–III of the rat RSG.

REFERENCES

Adams CE, Stitzel JA, Collins AC, Freedman R (2001) Alpha7-nicotinic receptor expression and the anatomical organization of hippocampal interneurons. Brain Res 922:180–190.

Aggleton JP (2010) Understanding retrosplenial amnesia: insights from animal studies. Neuropsychologia 48:2328–2338.

Aggleton JP, Brown MW (1999) Episodic memory, amnesia, and the hippocampal–anterior thalamic axis. Behav Brain Sci 22:425–444. discussion 444–489.

Aggleton JP, Pearce JM (2001) Neural systems underlying episodic memory: insights from animal research. Philos Trans R Soc Lond B Biol Sci 356:1467–1482.

Alkondon M, Albuquerque EX (2001) Nicotinic acetylcholine receptor alpha7 and alpha4beta2 subtypes differentially control GABAergic input to CA1 neurons in rat hippocampus. J Neurophysiol 86:3043–3055.

Alkondon M, Pereira EF, Wonnacott S, Albuquerque EX (1992) Blockade of nicotinic currents in hippocampal neurons defines methyllycaconitine as a potent and specific receptor antagonist. Mol Pharmacol 41:802–808.

Alkondon M, Pereira EF, Barbosa CT, Albuquerque EX (1997) Neuronal nicotinic acetylcholine receptor activation modulates gamma-aminobutyric acid release from CA1 neurons of rat hippocampal slices. J Pharmacol Exp Ther 283:1396–1411.

Alkondon M, Pereira EF, Albuquerque EX (1998) α-Bungarotoxin- and methyllycaconitine-sensitive nicotinic receptors mediate fast synaptic transmission in interneurons of rat hippocampal slices. Brain Res 810:257–263.

Alkondon M, Pereira EF, Eisenberg HM, Albuquerque EX (1999) Choline and selective antagonists identify two subtypes of nicotinic acetylcholine receptors that modulate GABA release from CA1 interneurons in rat hippocampal slices. J Neurosci 19:2693–2705.

Arnaiz-Cot JJ, González JC, Sobrado M, Baldelli P, Carbone E, Gandía L, García AG, Hernández-Guijo JM (2008) Allosteric modulation of alpha 7 nicotinic receptors selectively depolarizes hippocampal interneurons, enhancing spontaneous GABAergic transmission. Eur J Neurosci 27:1097–1110.

Buhler AV, Dunwiddie TV (2001) Regulation of the activity of hippocampal stratum oriens interneurons by alpha7 nicotinic acetylcholine receptors. Neuroscience 106:55–67.

Buhler AV, Dunwiddie TV (2002) Alpha7 nicotinic acetylcholine receptors on GABAergic interneurons evoke dendritic and

somatic inhibition of hippocampal neurons. J Neurophysiol 87:548–557.
Castro NG, Albuquerque EX (1995) α-Bungarotoxin-sensitive hippocampal nicotinic receptor channel has a high calcium permeability. Biophysics 68:516–524.
Cenquizca LA, Swanson LW (2007) Spatial organization of direct hippocampal field CA1 axonal projections to the rest of the cerebral cortex. Brain Res Rev 56:1–26.
Centeno ML, Henderson JA, Pau KY, Bethea CL (2006) Estradiol increases alpha7 nicotinic receptor in serotonergic dorsal raphe and noradrenergic locus coeruleus neurons of macaques. J Comp Neurol 497:489–501.
Chan J, Aoki C, Pickel VM (1990) Optimization of differential immunogold–silver and peroxidase labeling with maintenance of ultrastructure in brain sections before plastic embedding. J Neurosci Methods 33:113–127.
Christophe E, Roebuck A, Staiger JF, Lavery DJ, Charpak S, Audinat E (2002) Two types of nicotinic receptors mediate an excitation of neocortical layer I interneurons. J Neurophysiol 88:1318–1327.
Cooper BG, Mizumori SJ (1999) Retrosplenial cortex inactivation selectively impairs navigation in darkness. Neuroreport 10:625–630.
Cooper BG, Mizumori SJ (2001) Temporary inactivation of the retrosplenial cortex causes a transient reorganization of spatial coding in the hippocampus. J Neurosci 21:3986–4001.
Cooper BG, Manka TF, Mizumori SJ (2001) Finding your way in the dark: the retrosplenial cortex contributes to spatial memory and navigation without visual cues. Behav Neurosci 115:1012–1028.
Dajas-Bailador F, Wonnacott S (2004) Nicotinic acetylcholine receptors and the regulation of neuronal signalling. Trends Pharmacol Sci 25:317–324.
Dehkordi O, Millis RM, Dennis GC, Jazini E, Williams C, Hussain D, Jayam-Trouth A (2007) Expression of alpha-7 and alpha-4 nicotinic acetylcholine receptors by GABAergic neurons of rostral ventral medulla and caudal pons. Brain Res 1185:95–102.
Dominguez del Toro E, Juiz JM, Peng X, Lindstrom J, Criado M (1994) Immunocytochemical localization of the alpha 7 subunit of the nicotinic acetylcholine receptor in the rat central nervous system. J Comp Neurol 349:325–342.
Dougherty KD, Milner TA (1999) Cholinergic septal afferent terminals preferentially contact neuropeptide Y-containing interneurons compared to parvalbumin-containing interneurons in the rat dentate gyrus. J Neurosci 19:10140–10152.
Duffy AM, Zhou P, Milner TA, Pickel VM (2009) Spatial and intracellular relationships between the alpha7 nicotinic acetylcholine receptor and the vesicular acetylcholine transporter in the prefrontal cortex of rat and mouse. Neuroscience 161:1091–1103.
Eckenstein FP, Baughman RW, Quinn J (1988) An anatomical study of cholinergic innervation in rat cerebral cortex. Neuroscience 25:457–474.
Fabian-Fine R, Skehel P, Errington ML, Davies HA, Sher E, Stewart MG, Fine A (2001) Ultrastructural distribution of the alpha7 nicotinic acetylcholine receptor subunit in rat hippocampus. J Neurosci 21:7993–8003.
Finch DM, Derian EL, Babb TL (1984) Afferent fibers to rat cingulate cortex. Exp Neurol 83:468–485.
Frazier CJ, Buhler AV, Weiner JL, Dunwiddie TV (1998a) Synaptic potentials mediated via alpha-bungarotoxin-sensitive nicotinic acetylcholine receptors in rat hippocampal interneurons. J Neurosci 18:8228–8235.
Frazier CJ, Rollins YD, Breese CR, Leonard S, Freedman R, Dunwiddie TV (1998b) Acetylcholine activates an alpha-bungarotoxin-sensitive nicotinic current in rat hippocampal interneurons, but not pyramidal cells. J Neurosci 18:1187–1195.
Freedman R, Wetmore C, Strömberg I, Leonard S, Olson L (1993) Alpha-bungarotoxin binding to hippocampal interneurons: immunocytochemical characterization and effects on growth factor expression. J Neurosci 13:1965–1975.
Fujii S, Jia Y, Yang A, Sumikawa K (2000) Nicotine reverses GABAergic inhibition of long-term potentiation induction in the hippocampal CA1 region. Brain Res 863:259–265.
Gage SL, Keim SR, Simon JR, Low WC (1994) Cholinergic innervation of the retrosplenial cortex via the fornix pathway as determined by high affinity choline uptake, choline acetyltransferase activity, and muscarinic receptor binding in the rat. Neurochem Res 19:1379–1386.
Garden DL, Massey PV, Caruana DA, Johnson B, Warburton EC, Aggleton JP, Bashir ZI (2009) Anterior thalamic lesions stop synaptic plasticity in retrosplenial cortex slices: expanding the pathology of diencephalic amnesia. Brain 132:1847–1857.
Gaykema RP, Luiten PG, Nyakas C, Traber J (1990) Cortical projection patterns of the medial septum-diagonal band complex. J Comp Neurol 293:103–124.
Gilmor ML, Nash NR, Roghani A, Edwards RH, Yi H, Hersch SM, Levey AI (1996) Expression of the putative vesicular acetylcholine transporter in rat brain and localization in cholinergic synaptic vesicles. J Neurosci 16:2179–2190.
Gonzalo-Ruiz A, Morte L (2000) Localization of amino acids, neuropeptides and cholinergic markers in neurons of the septum-diagonal band complex projecting to the retrosplenial granular cortex of the rat. Brain Res Bull 52:499–510.
Gray R, Rajan AS, Radcliffe KA, Yakehiro M, Dani JA (1996) Hippocampal synaptic transmission enhanced by low concentrations of nicotine. Nature 383:713–716.
Gulledge AT, Kawaguchi Y (2007) Phasic cholinergic signaling in the hippocampus: functional homology with the neocortex? Hippocampus 17:327–332.
Gulyás AI, Szabó GG, Ulbert I, Holderith N, Monyer H, Erdélyi F, Szabó G, Freund TF, Hájos N (2010) Parvalbumin-containing fast-spiking basket cells generate the field potential oscillations induced by cholinergic receptor activation in the hippocampus. J Neurosci 30:15134–15145.
Han ZY, Zoli M, Cardona A, Bourgeois JP, Changeux JP, Le Novère N (2003) Localization of [3H]nicotine, [3H]cytisine, [3H]epibatidine, and [125I]alpha-bungarotoxin binding sites in the brain of *Macaca mulatta*. J Comp Neurol 461:49–60.
Harker KT, Whishaw IQ (2002) Impaired spatial performance in rats with retrosplenial lesions: importance of the spatial problem and the rat strain in identifying lesion effects in a swimming pool. J Neurosci 22:1155–1164.
Heckers S, Ohtake T, Wiley RG, Lappi DA, Geula C, Mesulam MM (1994) Complete and selective cholinergic denervation of rat neocortex and hippocampus but not amygdala by an immunotoxin against the p75 NGF receptor. J Neurosci 14:1271–1289.
Herber DL, Severance EG, Cuevas J, Morgan D, Gordon MN (2004) Biochemical and histochemical evidence of nonspecific binding of alpha7nAChR antibodies to mouse brain tissue. J Histochem Cytochem 52:1367–1376.
Ichinohe N (2012) Small-scale module of the rat granular retrosplenial cortex: an example of the minicolumn-like structure of the cerebral cortex. Front Neuroanat 5:69.
Ichinohe N, Rockland KS (2002) Parvalbumin positive dendrites co-localize with apical dendritic bundles in rat retrosplenial cortex. Neuroreport 13:757–761.
Irizarry MC, Soriano F, McNamara M, Page KJ, Schenk D, Games D, Hyman BT (1997) Abeta deposition is associated with neuropil changes, but not with overt neuronal loss in the human amyloid precursor protein V717F (PDAPP) transgenic mouse. J Neurosci 17:7053–7059.
Ji D, Dani JA (2000) Inhibition and disinhibition of pyramidal neurons by activation of nicotinic receptors on hippocampal interneurons. J Neurophysiol 83:2682–2690.
Ji D, Lape R, Dani JA (2001) Timing and location of nicotinic activity enhances or depresses hippocampal synaptic plasticity. Neuron 31:131–141.
Jinno S, Klausberger T, Marton LF, Dalezios Y, Roberts JD, Fuentealba P, Bushong EA, Henze D, Buzsáki G, Somogyi P

(2007) Neuronal diversity in GABAergic long-range projections from the hippocampus. J Neurosci 27:8790–8804.
Jones IW, Wonnacott S (2004) Precise localization of alpha7 nicotinic acetylcholine receptors on glutamatergic axon terminals in the rat ventral tegmental area. J Neurosci 24:11244–11252.
Jones IW, Wonnacott S (2005) Why doesn't nicotinic ACh receptor immunoreactivity knock out? Trends Neurosci 28:343–345.
Jones S, Yakel JL (1997) Functional nicotinic ACh receptors on interneurones in the rat hippocampus. J Physiol 504:603–610.
Kawaguchi Y (1997) Selective cholinergic modulation of cortical GABAergic cell subtypes. J Neurophysiol 78:1743–1747.
Kawaguchi Y, Kondo S (2002) Parvalbumin, somatostatin and cholecystokinin as chemical markers for specific GABAergic interneuron types in the rat frontal cortex. J Neurocytol 31:277–287.
Kawai H, Zago W, Berg DK (2002) Nicotinic alpha7 Receptor Clusters on Hippocampal GABAergic Neurons: Regulation by Synaptic Activity and Neurotrophins. J Neurosci 22:7903–7912.
Krenz I, Kalkan D, Wevers A, de Vos RA, Steur EN, Lindstrom J, Pilz K, Nowacki S, Schütz U, Moser N, Witter B, Schröder H (2001) Parvalbumin-containing interneurons of the human cerebral cortex express nicotinic acetylcholine receptor proteins. J Chem Neuroanat 21:239–246.
Lee S, Hjerling-Leffler J, Zagha E, Fishell G, Rudy B (2010) The largest group of superficial neocortical GABAergic interneurons expresses ionotropic serotonin receptors. J Neurosci 30:16796–16808.
Letzkus JJ, Wolff SB, Meyer EM, Tovote P, Courtin J, Herry C, Lüthi A (2011) A disinhibitory microcircuit for associative fear learning in the auditory cortex. Nature 480:331–335.
Levy RB, Aoki C (2002) Alpha7 nicotinic acetylcholine receptors occur at postsynaptic densities of AMPA receptor-positive and -negative excitatory synapses in rat sensory cortex. J Neurosci 22:5001–5015.
Lysakowski A, Wainer BH, Bruce G, Hersh LB (1989) An atlas of the regional and laminar distribution of choline acetyltransferase immunoreactivity in rat cerebral cortex. Neuroscience 28:291–336.
Maddock RJ (1999) The retrosplenial cortex and emotion: new insights from functional neuroimaging of the human brain. Trends Neurosci 22:310–316.
McGowan E, Sanders S, Iwatsubo T, Takeuchi A, Saido T, Zehr C, Yu X, Uljon S, Wang R, Mann D, Dickson D, Duff K (1999) Amyloid phenotype characterization of transgenic mice overexpressing both mutant amyloid precursor protein and mutant presenilin 1 transgenes. Neurobiol Dis:231–244.
McQuiston AR, Madison DV (1999) Nicotinic receptor activation excites distinct subtypes of interneurons in the rat hippocampus. J Neurosci 9:2887–2896.
Miyashita T, Rockland KS (2007) GABAergic projections from the hippocampus to the retrosplenial cortex in the rat. Eur J Neurosci 26:1193–1204.
Miyoshi G, Hjerling-Leffler J, Karayannis T, Sousa VH, Butt SJ, Battiste J, Johnson JE, Machold RP, Fishell G (2010) Genetic fate mapping reveals that the caudal ganglionic eminence produces a large and diverse population of superficial cortical interneurons. J Neurosci 30:1582–1594.
Morales M, Hein K, Vogel Z (2008) Hippocampal interneurons co-express transcripts encoding the alpha7 nicotinic receptor subunit and the cannabinoid receptor 1. Neuroscience 152:70–81.
Mufson EJ, Pandya DN (1984) Some observations on the course and composition of the cingulum bundle in the rhesus monkey. J Comp Neurol 225:31–43.
Murakami K, Yokofujita J, Kuroda M (2000) Non-cholinergic projections from basal forebrain to medial limbic cortex of rat. Kaibogaku Zasshi 75:285–297.
Paxinos G, Watson C (1998) The rat brain in stereotaxic coordinates. Orlando: Academic Press.
Pengas G, Hodges JR, Watson P, Nestor PJ (2010) Focal posterior cingulate atrophy in incipient Alzheimer's disease. Neurobiol Aging 31:25–33.
Platt B, Riedel G (2011) The cholinergic system, EEG and sleep. Behav Brain Res 221:499–504.
Poirier GL, Amina E, Gooda MA, Aggleton JP (2011) Early-onset dysfunction of retrosplenial cortex precedes overt amyloid plaque formation in Tg2576 mice. Neuroscience 174:71–83.
Poorthuis RB, Bloem B, Schak B, Wester J, de Kock CP, Mansvelder HD (2013) Layer-specific modulation of the prefrontal cortex by nicotinic acetylcholine receptors. Cereb Cortex 23:148–161.
Porter JT, Cauli B, Tsuzuki K, Lambolez B, Rossier J, Audinat E (1999) Selective excitation of subtypes of neocortical interneurons by nicotinic receptors. J Neurosci 19:5228–5235.
Price JL, Stern R (1983) Individual cells in the nucleus basalis-diagonal band complex have restricted axonal projections to the cerebral cortex in the rat. Brain Res 269:352–356.
Ramos-Moreno T, Galazo MJ, Porrero C, Martínez-Cerdeño V, Clascá F (2006) Extracellular matrix molecules and synaptic plasticity: immunomapping of intracellular and secreted Reelin in the adult rat brain. Eur J Neurosci 23:401–422.
Robertson RT, Kaitz SS (1981) Thalamic connections with limbic cortex. I. Thalamocortical projections. J Comp Neurol 195:501–525.
Robertson RT, Baratta J, Yu J, LaFerla FM (2009) Amyloid-beta expression in retrosplenial cortex of triple transgenic mice: relationship to cholinergic axonal afferents from medial septum. Neuroscience 164:1334–1346.
Rudy B, Fishell G, Lee S, Hjerling-Leffler J (2011) Three groups of interneurons account for nearly 100% of neocortical GABAergic neurons. Dev Neurobiol 71:45–61.
Rye DB, Wainer BH, Mesulam MM, Mufson EJ, Saper CB (1984) Cortical projections arising from the basal forebrain: a study of cholinergic and noncholinergic components employing combined retrograde tracing and immunohistochemical localization of choline acetyltransferase. Neuroscience 13:627–643.
Saper CB (1984) Organization of cerebral cortical afferent systems in the rat. II. Magnocellular basal nucleus. J Comp Neurol 222:313–342.
Schafer MK, Eiden LE, Weihe E (1998) Cholinergic neurons and terminal fields revealed by immunohistochemistry for the vesicular acetylcholine transporter. Neuroscience 84:331–359.
Senut MC, Menetrey D, Lamour Y (1989) Cholinergic and peptidergic projections from the medial septum and the nucleus of the diagonal band of Broca to cingulate cortex and olfactory bulb: a combined wheatgerm agglutinin-apohorseradish peroxidase-gold immunohistochemical study. Neuroscience 30:385–403.
Sesack SR, Hawrylak VA, Melchitzky DS, Lewis DA (1998) Dopamine innervation of a subclass of local circuit neurons in monkey prefrontal cortex: ultrastructural analysis of tyrosine hydroxylase and parvalbumin immunoreactive structures. Cereb Cortex 8:614–622.
Shibata H, Kondo S, Naito J (2004) Organization of retrosplenial cortical projections to the anterior cingulate, motor, and prefrontal cortices in the rat. Neurosci Res 49:1–11.
Slomianka L, Geneser FA (1991) Distribution of acetylcholinesterase in the hippocampal region of the mouse: I. Entorhinal area, parasubiculum, retrosplenial area, and presubiculum. J Comp Neurol 303:339–354.
Son JH, Winzer-Serhan UH (2008) Expression of neuronal nicotinic acetylcholine receptor subunit mRNAs in rat hippocampal GABAergic interneurons. J Comp Neurol 511:286–299.
Sorensen KE (1980) Ipsilateral projection from the subiculum to the retrosplenial cortex in the guinea pig. J Comp Neurol 193:893–911.
Sripanidkulchai K, Wyss JM (1986) Thalamic projections to retrosplenial cortex in the rat. J Comp Neurol 254:143–165.
Takeuchi A, Irizarry MC, Duff K, Saido TC, Hsiao Ashe K, Hasegawa M, Mann DM, Hyman BT, Iwatsubo T (2000) Erratum in age-related amyloid beta deposition in transgenic mice overexpressing both Alzheimer mutant presenilin 1 and amyloid beta precursor protein Swedish mutant is not associated with global neuronal loss. Am J Pathol 157:331–339. 157:1413 (erratum).

Tengelsen LA, Robertson RT, Yu J (1992) Basal forebrain and anterior thalamic contributions to acetylcholinesterase activity in granular retrosplenial cortex of rats. Brain Res 594:10–18.

van Groen T, Wyss JM (1990) Connections of the retrosplenial granular a cortex in the rat. J Comp Neurol 300:593–606.

van Groen T, Wyss JM (1992) Projections from the laterodorsal nucleus of the thalamus to the limbic and visual cortices in the rat. J Comp Neurol 324:427–448.

van Groen T, Kadish I, Wyss JM (2004) Retrosplenial cortex lesions of area Rgb (but not of area Rga) impair spatial learning and memory in the rat. Behav Brain Res 154:483–491.

Vann SD, Aggleton JP (2002) Extensive cytotoxic lesions of the rat retrosplenial cortex reveal consistent deficits on tasks that tax allocentric spatial memory. Behav Neurosci 116:85–94.

Vann SD, Kristina Wilton LA, Muir JL, Aggleton JP (2003) Testing the importance of the caudal retrosplenial cortex for spatial memory in rats. Behav Brain Res 140:107–118.

Vann SD, Aggleton JP, Maguire EA (2009) What does the retrosplenial cortex do? Nat Rev Neurosci 10:792–802.

Villain N, Desgranges B, Viader F, de la Sayette V, Mézenge F, Landeau B, Baron JC, Eustache F, Chételat G (2008) Relationships between hippocampal atrophy, white matter disruption, and gray matter hypometabolism in Alzheimer's disease. J Neurosci 28:6174–6181.

Vogt BA, Miller MW (1983) Cortical connections between rat cingulate cortex and visual, motor, and postsubicular cortices. J Comp Neurol 216:192–210.

Vogt BA, Peters A (1981) Form and distribution of neurons in rat cingulated cortex: areas 32, 24 and 29. J Comp Neurol 195:603–625. 200:461 (erratum).

Vogt LJ, Vogt BA, Sikes RW (1992) Limbic thalamus in rabbit: architecture, projections to cingulated cortex and distribution of muscarinic acetylcholine, GABAA, and opioid receptors. J Comp Neurol 319(2):205–217.

Vogt BA, Vogt LJ, FarBer NB (2004) Cingulate cortex and disease models. In: Paxinos G, editor. The rat nervous system. Tokyo: Elsevier Academic Press. p. 705–727.

Wang HY, Lee DH, D'Andrea MR, Peterson PA, Shank RP, Reitz AB (2000a) Beta-Amyloid(1–42) binds to alpha7 nicotinic acetylcholine receptor with high affinity. Implications for Alzheimer's disease pathology. J Biol Chem 275:5626–5632.

Wang HY, Lee DH, Davis CB, Shank RP (2000b) Amyloid peptide Abeta(1–42) binds selectively and with picomolar affinity to alpha7 nicotinic acetylcholine receptors. J Neurochem 75:1155–1161.

White TD, Tan AM (1991) Functional connections of the rat medial cortex and basal forebrain: an in vivo intracellular study. Neuroscience 44:571–583.

Wyss JM, Van Groen T (1992) Connections between the retrosplenial cortex and the hippocampal formation in the rat: a review. Hippocampus 2:1–11.

(Accepted 15 August 2013)
(Available online 25 August 2013)